Molecular basis for optical clearing of collagenous tissues

Jason M. Hirshburg
Krishnakumar M. Ravikumar
Wonmuk Hwang
Alvin T. Yeh
Texas A&M University
Department of Biomedical Engineering
337 Zachry Engineering Center
3120 TAMU
College Station, Texas 77843

Abstract. Molecular interactions of optical clearing agents were investigated using a combination of molecular dynamics (MD) simulations and optical spectroscopy. For a series of sugar alcohols with low to high optical clearing potential, Raman spectroscopy and integrating sphere measurements were used to quantitatively characterize tissue water loss and reduction in light scattering following agent exposures. The rate of tissue water loss was found to correlate with agent optical clearing potential, but equivalent tissue optical clearing was measured in native and fixed tissue *in vitro*, given long-enough exposure times to the polyol series. MD simulations showed that the rate of tissue optical clearing correlated with the preferential formation of hydrogen bond bridges between agent and collagen. Hydrogen bond bridge formation disrupts the collagen hydration layer and facilitates replacement by a chemical agent to homogenize tissue refractive index. However, the reduction in tissue light scattering did not correlate with the agent index of refraction. Our results suggest that a necessary property of optical clearing agents is hyperosmolarity to tissue, but that the most effective agents with the highest rates of optical clearing are a subset with the highest collagen solubilities. [DOI: 10.1117/1.3484748]

Keywords: collagen; hydrogen bond bridge; hyperosmotic agent; molecular dynamics simulations; sugar-alcohol; sugar.

Paper 10123R received Mar. 15, 2010; revised manuscript received Jul. 7, 2010; accepted for publication Jul. 19, 2010; published online Sep. 7, 2010.

1 Introduction

Biocompatible chemical agents have been shown to induce a temporary and reversible reduction in tissue light scattering.[1,2] With concentrated sugar alcohols, such as sorbitol, and sugars, such as high fructose corn syrup (HFCS), light scattering can be reduced as much as fivefold. These chemical agents have been observed to be most effective *in vitro* when applied directly to the mesenchyme (e.g., the dermis of skin, and less so when applied topically). The putative mechanism of optical clearing is index matching of tissue light scatterers via optical immersion.[1] Index matching as a mechanism is intriguing because, ultimately, a reduction in light scattering must coincide with a homogenization of the index of refraction. Yet, as a physical parameter, index of refraction of potential optical clearing agents cannot be used to predict "clearing" effectiveness. Tissue dehydration has also been proposed as a mechanism of optical clearing.[3] Water makes up a substantial proportion of tissue weight and has an index of refraction significantly different from that of insoluble biological constituents. However, chemical agent osmolarity cannot be used as a predictor of its optical clearing potential. A better understanding of how the index of refraction is homogenized in optically cleared tissue could lead to a rational basis for designing effective, clinically applicable formulations.[4]

Previously, it has been shown at microscopic and ultrastructural length scales that glycerol, a prototypical optical clearing agent, destabilizes high-order collagen structures and that this effect coincides with agent-induced tissue transparency.[5–7] It has been suggested that collagen destabilization was due to the chemical agent's ability to screen noncovalent, hydrophilic, attractive forces. These same forces drive collagen fibrillogenesis from solution and have been characterized in the presence of sugars and sugar alcohols.[8] We introduced collagen solubility as a measure of a chemical agent's ability to screen noncovalent forces and correlated it with tissue optical clearing for a series of polyols and sugars.[5,9] These studies suggested that, of the chemical agents in the series, their optical clearing potential (and collagen solubility) could be grouped by chain length and locations of hydroxyl groups within the molecule. More specifically for sugar alcohols, optical clearing potential for the series could be grouped by chain length, in increasing order, as two-carbon backbone (ethylene glycol), three- to five-carbon backbone (glycerol to xylitol), and six-carbon backbone (sorbitol). Herein, we examine the interactions between clearing agents and collagen using a combination of molecular dynamics (MD) simulations and experiments to elucidate the roles of collagen solubility, refractive index matching, and dehydration in skin optical clearing. Our results suggest that the po-

Address all correspondence to: Alvin T. Yeh, Texas A&M University, Department of Biomedical Engineering, 337 Zachry Engineering Center, 3120 TAMU, College Station, Texas 77843. Tel: 979-845-5468; Fax: 979-845-4450. E-mail: ayeh@tamu.edu

1083-3668/2010/15(5)/055002/8/$25.00 © 2010 SPIE

sition of hydroxyl groups on alcohols impose steric constraints for forming surface bridges on the collagen triple helix; thus, it is an important factor in determining its optical clearing properties. Combined with experimental results, our simulation provides an atomistic picture for the nonlinear trend in optical clearing properties of alcohols as their chain length increases.

2 Materials and Methods

2.1 *Molecular Dynamics Simulations*

MD simulations were used to enhance our understanding of chemical agent-collagen interactions and the roles that these interactions may have on tissue optical clearing. In MD simulation, a system such as a protein structure is set up and atomic forces including bonded and nonbonded interactions are calculated at each integration time step. Integrating the corresponding Newton's equation of motion yields the trajectories of atoms in the system.[10] MD simulation provides the molecular basis to understand and interpret experimental results that are difficult to gain from experiments alone.

For simulation, we used CHARMM version 34 with param22 force field.[11] The generalized Born with a simple switching implicit solvent model was used to account for solvation effects.[12] The main focus of our simulation was finding geometric constraints and propensities of various polyols in forming hydrogen bond bridges on collagen surfaces that are determined mainly by the structures of these molecules. Thus, using an implicit solvent model rather than a more computationally demanding explicit water simulation was sufficient for our purpose.

A native collagen molecule is a 300-nm-long triple helix composed of multiple domains. Simulating this long molecule would be computationally very demanding. We thus used two collagen mimetic peptides that are representative of the collagen molecule; 1BKV (Protein Data Bank ID) and a regular GPO peptide, $[(GPO)_{10}]_3$ (G, glycine; P, proline; and O, hydroxyproline) for simulations. Peptide GPO is known to form the most stable triple helical motif of collagen.[13,14] On the other hand, peptide 1BKV has a middle region devoid of Pro and Hyp, which is less stable but functionally important for collagen cleavage.[15,16] Using simulations of these structurally and functionally relevant sequences, it is possible to infer polyol interactions with native collagen. The backbone structure of the GPO peptide was built using the THeBuScr collagen building script.[17] Side chain atoms were added to the backbone using the existing amino acid topology files and systematically energy minimized as done previously[16] to get the final structure. Polar hydrogens were added to the peptides using the HBUILD facility in CHARMM.[18] Parameters for hydroxyproline were added from a previous study.[19] The final structure of collagen triple helix constructed using this method agreed very well with existing x-ray data.[20] Structures of the sugar alcohols (glycerol, xylitol, and sorbitol) were built from the already existing lipid topology and parameter files.

Each alcohol was simulated with either 1BKV or the GPO triple helix, making a total of six separate simulation runs. In each simulation, alcohol molecules were placed randomly around the peptide at a radial distance of 12.0 Å from the cylindrical axis of the triple helix. Owing to their bigger molecular structures, only 12 molecules of xylitol and sorbitol were placed around the peptide, while 20 glycerol molecules were used. The systems were first energy minimized to remove close contacts and then heated at the rate of 5 K/ps for 60 ps to 300 K. The systems were then equilibrated for 40 ps at 300 K. Each production run lasted 600 ps, where the Verlet integration algorithm was used with a time step of 2.0 fs. As the system was in a microcanonical ensemble (constant total energy), binding of alcohols to collagen resulted in a slight increase of temperature due to the loss of potential energy. The maximum variation was seen in the case of sorbitol simulation, where the average temperature was 309 ± 6 K. Note that this does not affect our results, since we only study the hydrogen bonding modes of different alcohols, which will not change appreciably within the range of temperatures.

Coordinates were saved every 1 ps. To prevent the drift of the peptide outside the simulation boundary, harmonic constraints (spring constant=2 kcal/[mol Å^2]) were applied on all peptide atoms to their original positions during heating and equilibration. During the production run, harmonic constraints were applied only on backbone amide nitrogen, alpha carbon, and carboxylic carbon atoms, leaving the rest of the atoms, including side chains, to freely interact with the alcohol molecules. To prevent diffusion of alcohol molecules away from the peptide, a cylindrical boundary 40 Å diam was imposed around the peptide, which activated a radial harmonic potential when alcohol molecules moved beyond the boundary, with a spring constant of 1 kcal/[mol Å^2].

Hydrogen bonds were defined using a distance cutoff of 2.4 Å[21] and a hydrogen bond bridge, which we will simply refer as a bridge, was defined to be formed if an alcohol molecule was simultaneously hydrogen bonded to two atoms of the collagen triple helix. We analyzed the propensities of the hydroxyl groups of alcohols to form bridges with collagen peptides as follows. Bridges formed by alcohol –OH groups on adjacent carbon positions were labeled type I; bridges formed between positions separated by one carbon were labeled type II; and so on. Bond multiplicity (n) of each type was also considered. For example in the three-carbon glycerol molecule, a type I bridge with collagen can involve hydroxyl groups in positions {1,2} or {2,3} leading to an n value of 2, while type II bridge [Fig. 1(a)] involves {1,3} hydroxyl groups with an n value of 1. We counted the number of alcohol bridges every 1 ps for the entire simulation (600 ps), and the percentage of different types of bridges are shown in Fig. 2. Because of a higher number of hydrogen bonding groups in 1BKV, there was a slightly higher number of bridges. However, the preferences for different types of bridges were very similar between GPO and 1BKV, and only their sum is shown in Fig. 2 for clarity. Also, to test whether 600 ps provided sufficient sampling, we compared bridge formation for the first and last 300 ps, which showed identical trends in the preference for the bridge types and in differences among various polyols.

2.2 *Tissue Preparation for Raman Spectroscopy*

Ex vivo rodent skin (3–6-wk-old Sprague-Dawley) was cut into 1.0×1.0 cm^2 samples using surgical scissors. Subcutaneous fat was removed using a razorblade, and the sample was stored in 99.9% deuterium oxide for 24 h. Deuterium

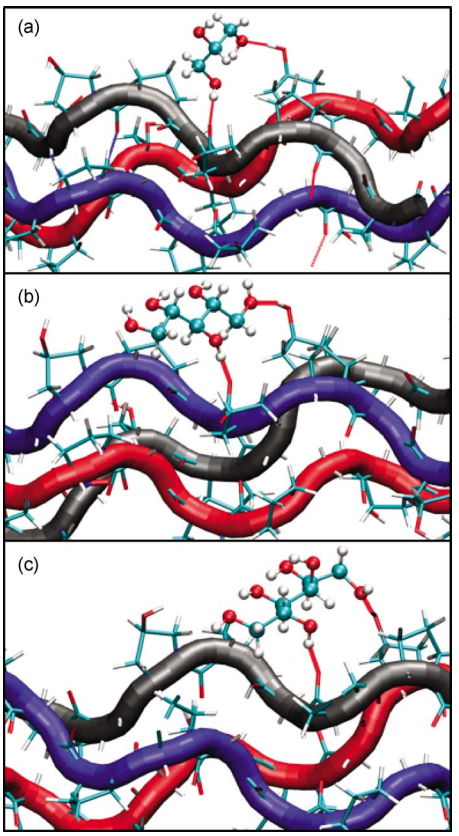

Fig. 1 Typical hydrogen bond bridges in alcohols. Bridge of –OH groups between (a) one and three carbon positions (type II) in glycerol, (b) one and three carbon positions (type II) in xylitol, and (c) one and five carbon positions (type IV) in sorbitol. Higher bridge types, as in (c), span further across the collagen surface and can potentially disrupt collagen-collagen and collagen-water interactions better than lower bridge types.

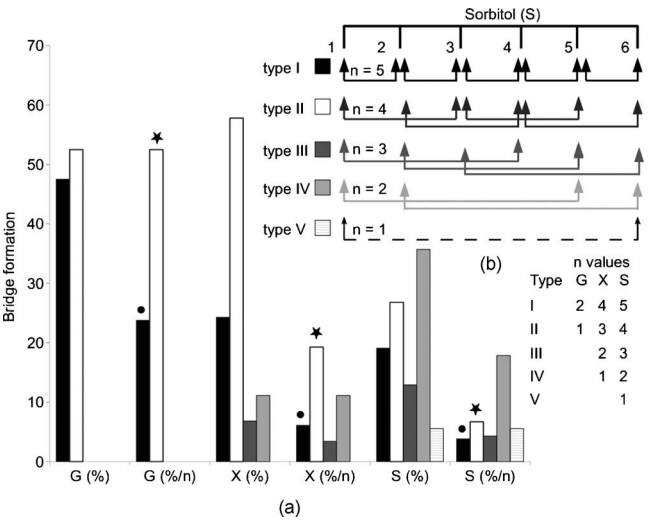

Fig. 2 Propensity of hydrogen bond bridge formation. (Inset) Sorbitiol molecule stick diagram with six –OH groups (one on each carbon atom). Gray-scale bonding pattern shown by arrows indicates the number of different variations or multiplicity (n) of hydrogen bond bridges for different bridge types. For example, type IV bridge between –OH groups separated by five carbon atoms can form in two ways (n=2). (a) Bar graph of percent bridge formation and percent averaged by multiplicity for each bridge type between alcohols and collagen (%/n). Circle and star indicate hydrogen bond bridges favors –OH groups in 1,3 over 1,2 positions. (b) Bond multiplicity (n) of glycerol (G), xylitol (X), and sorbitol (S).

oxide (D_2O) quickly replaces water in native rodent skin and provides a unique Raman band (2250–2800 cm^{-1}) not found in native or fixed rodent skin. The unique Raman signature of D_2O allows quantitative examination of the dehydration of native and fixed rodent skin due to clearing agents. D_2O loss from clearing agent–induced dehydration resulted in decreasing D_2O Raman band areas. Following immersion in D_2O, the excised skin was randomly divided into two groups: native and fixed. Fixation was carried out in 0.10, 0.25, and 0.50% vol/vol glutaraldehyde in D_2O for 48 h at pH 7.2, 27 °C. After chemical treatment, excess glutaraldehyde was rinsed off using D_2O at 27 °C.

2.3 *Dehydration of Fixed Rodent Skin*

Raman spectra were collected for native and fixed rodent skin before and after immersion in 3.5 M concentrations of the clearing agents ethylene glycol, glycerol, and HFCS.

2.4 *Kinetics of Dehydration*

The kinetics of dehydration were compared between 1,2- and 1,3-propanediol (3.5 M). Native and glutaraldehyde fixed (0.10, 0.25, and 0.50% vol/vol) rodent skin in D_2O at pH 7.2, 27 °C was immersed in each clearing agent with D_2O Raman band measurement at 5 min intervals for a total of 20 min for native skin and 10 min intervals for a total of 120 min for fixed skin.

2.5 *Raman Spectroscopy*

Raman spectra were collected using a LabRam Raman spectrometer (Jobin-Yvon-Horriba) comprising an Olympus BX41 confocal microscope (200-μm pinhole), 50× objective, 633 nm excitation laser, and CCD detector. Samples were placed on a glass slide, and care was taken to prevent heating and dehydration of the sample from the laser source or air. Keeping the laser source exiting the objective at or below 3 mW did not change the Raman spectra and prevented heating of the sample.[22,23] The spectra were recorded using a 300-grooves/mm grating, 5 scans per spectra with an integration time of 15 s per scan. Ten measurements were taken from the dermal side per skin sample, and each spectrum averaged to accommodate the natural heterogeneity of the dermis. Baselines were adjusted using an eighth-order polynomial fit, and spectra were normalized to phenylalanine aromatic peak at 1001 cm^{-1} to account for changes in tissue optical properties before determining area of OD Raman band (2200–2800 cm^{-1}).

2.6 *Bulk Skin Optical Measurements*

Ex vivo rodent skin (3–6-wk-old Sprague-Dawley) was cut into 1.5×1.5 cm^2 samples using surgical scissors. Subcutaneous fat was removed using a razor blade, and rodent skin was stored in 1×PBS at 4 °C. Experiments were performed within 24 h. Volume-matched solutions of each clearing agent to that of the skin sample were applied to the dermal side. The

chemical agents were applied for a total of 45 min and removed carefully with Kimwipes™ prior to transmittance and reflectance measurements. Skin thickness ($\sim$600 μm) was measured using a micrometer (Mitutoyo, Aurora, Illinois) after the sample had been placed between two glass slides of known thickness. The slides were secured using binder clips to ensure constant pressure on each skin sample.

An integrating sphere (Labsphere, North Sutton, New Hampshire) was used to determine the transmittance and reflectance of 635 nm laser diode light in rodent skin samples.[24,25] The skin/glass combination was placed at the entrance and exit ports of the integrating sphere for transmittance and reflectance measurements, respectively. For transmittance measurements, the exit port was covered using a spectralon-coated port plug (99% reflectance). Light measurements were conducted using a silicon photodiode (Labsphere) connected to an oscilloscope (Tektronix, Beaverton, Oregon). System calibration was performed using neutral density filters and reflectance standards (Labsphere). The inverse adding-doubling method[23] was used to calculate the reduced scattering coefficient, μ_s', for each skin sample before and after (45 min) clearing-agent application. Reduced scattering ratio (RSR), defined as the ratio of μ_s' before and after clearing agent application, was used to quantify the relation between μ_s' and chemical agent optical clearing potential (OCP).

MATLAB software (MathWorks, Natick, Massachusetts) was used to perform a one-way analysis of covariance (ANCOVA) test on the RSR data of rodent skin to test for statistically significant differences in the linear regression for each chemical agent. The overall RSR data were found to be dependent on chemical type (categorical variable) and concentration (continuous variable). The change in RSR for each clearing agent at a given concentration was assumed to be normally distributed. Analysis of the chemical agent with the need to control for the covariate (concentration) called for the use of ANCOVA. An F-test suggested that RSR mean values were significantly different, and t-tests were performed to compare the effects of the individual chemicals. The Scheffes multiple-comparison procedure was used to correct for the error associated with the large number of comparisons.[26]

3 Results

Our previous studies demonstrated that optical clearing potential and collagen solubility are correlated and, for sugar alcohols, depend on chain length in a "quantized" manner. For the series of sugar alcohols from ethylene glycol to sorbitol, OCP did not vary linearly with chain length, but rather exhibited "jumps" in clearing efficacy from ethylene glycol (two carbon) to glycerol (three carbon) to sorbitol (six carbon). In other words, for the same reduction in tissue scattering, the concentration of ethylene glycol was double that of glycerol and four times that of sorbitol. From the correlated collagen solubility and optical clearing data, it was hypothesized that effective chemical agents reduced collagen stabilizing hydrophilic forces by disrupting the hydration shell, thereby destabilizing higher-order (quaternary) structures of collagen.[5,9,27]

To understand the hydrogen bonding interactions of alcohols on the collagen surface, we performed MD simulations of collagen peptides 1BKV (containing imino-poor domain) and GPO (imino-rich) with glycerol, xylitol, and sorbitol. Hydroxyl groups of alcohols can form hydrogen bonds with collagen atoms and can displace water molecules in the hydration shell. It is expected that the disruption of the hydration shell is greater if the alcohol bridges span more extensively across the collagen surface (Fig. 1). Thus, propensity to form a bridge was hypothesized to be an important factor in optical clearing.

Bridging propensities of hydroxyl groups in glycerol, xylitol and sorbitol are shown in Fig. 2. Bridges were categorized by the positions of the participating hydroxyl groups. Type I bridges were formed with hydroxyl groups on adjacent carbon atoms (hydroxyl positions {1,2}, {2,3}, {3,4}, etc.); type II bridges were formed with hydroxyl groups separated by one carbon atom (hydroxyl positions {1,3}, {2,4}, etc.); type III bridges were formed with hydroxyl groups separated by two carbon atoms ({1,4}, {2,5}, etc.); and so on. Note that higher bridge type numbers can screen collagen-collagen and collagen-water interactions more effectively than lower bridge-type numbers (Fig. 1).

Figure 2 shows the fraction of different bridge types along with the normalized values based on the multiplicity (n) of each bridge type. Depending on the separations of hydroxyl groups, certain bridge types have higher propensities to form. For all alcohols in the MD simulation, type II bridges were more favored than type I bridges (indicated by the star and circle in Fig. 2). Xylitol and sorbitol, which have more than three hydroxyl groups, indicate a preference for type II and type IV bridges compared to type I or type III bridges. The difference between xylitol and sorbitol is their preference for type II and type IV bridges. While xylitol, like glycerol, prefers type II bridges [Figs. 1(a) and 1(b)], sorbitol prefers to form type IV bridges. Although more tests are necessary to clarify the above behavior, it provides a plausible explanation for similar optical clearing properties of xylitol and glycerol. Type IV bridges of sorbitol, on the other hand, span across the surface of the collagen triple helix, thereby screening collagen-water interactions much more effectively than xylitol.

To measure the kinetics of optical clearing and the effect of fixatives, we carried out a series of experiments quantifying tissue dehydration and optical properties. In previous studies, chemical agents exhibited statistically differing clearing efficacies after 1-h exposures in native skin, whereas formalin and glutaraldehyde fixation was shown to limit clearing.[5,7,9] Cross-linking fixatives increase water retention in collagenous tissues and potentially limit clearing agent infiltration.[22,23] We characterized tissue dehydration by chemical agents as a function of fixative concentration utilizing the unique Raman band of D_2O.

Deuterium oxide (D_2O) is freely interchangeable with water in skin and exhibits an OD Raman band from 2200 to 2800 cm^{-1}. Skin fixed in 0.10%, 0.25%, and 0.50% glutaraldehyde in D_2O was immersed in 3.5 M ethylene glycol, glycerol, and HFCS for 1 h. The fraction of D_2O remaining in fixed skin is shown in Fig. 3. Raman OD band areas are presented as a percentage of the initial, fully hydrated skin D_2O peak area. (The aromatic phenylalanine Raman band was used as a reference to account for changes in tissue optical properties.) OD band area fell in response to dehydration. Each clearing agent fully removed all measurable D_2O from

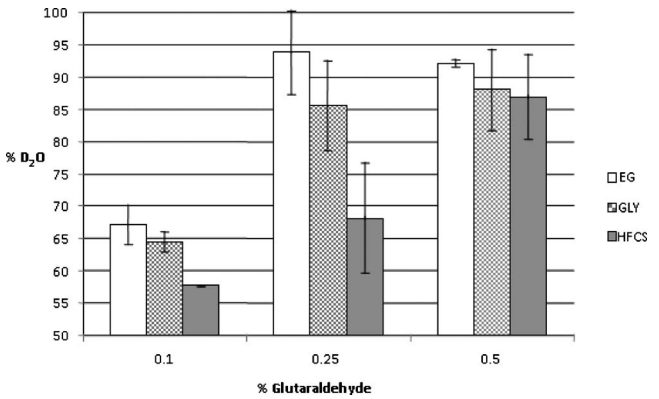

Fig. 3 Percent D_2O remaining in fixed skin after immersion for 1 h in ethylene glycol, glycerol, and HFCS. Increases in glutaraldehyde concentration lead to greater water retention.

native skin after 1 h (data not shown). The fraction of D_2O retained after 1-h exposure to chemical agents increased with increasing glutaraldehyde concentration fixation. HFCS was the most effective dehydrating agent followed by glycerol and ethylene glycol. This finding is consistent with previously reported studies that found reduced water exchange in glutaraldehyde fixed tissues.[22,23]

The kinetics of skin dehydration due to clearing agents is shown in Fig. 4. Clearing agents 1,2- and 1,3-propanediol were chosen for testing because of their identical molecular weight, similar refractive index, and osmolality, but factor of 2 difference in optical clearing potential (1,2- half that of 1,3-propanediol).[5] Native, 0.10%, 0.25%, and 0.50% glutaraldehyde/D_2O fixed rodent skin were dehydrated for 120 min by 1,2- and 1,3-propanediol. After 10 min of immersion in 3.5 M 1,3-propanediol, native rodent skin had a significantly reduced D_2O concentration compared to that immersed in 1,2-propanediol [Fig. 4(a)]. 0.10% glutaraldehyde fixed skin showed a similar, but delayed trend with 1,3-propanediol exhibiting greater dehydration effects 20 min after application [Fig. 4(b)]. Rodent skin fixed with higher concentrations of glutaraldehyde (0.25 and 0.50%) showed more D_2O retention with little difference between the two propanediols in water-removing capacity [Figs. 4(c) and 4(d)].

Optical clearing ability for a series of sugar alcohols and propanediols in 4% glutaraldehyde [pH 7.2 in phosphate buffered saline (PBS)] fixed rodent skin was measured after immersion for 24 h. RSR before and after immersion[5] was calculated as a function of agent concentration (Fig. 5). Immersion in all agents for 24 h was sufficient to induce clearing in fixed tissue. Beyond 24 h, all agents reduced tissue light scattering nearly equivalently with an optical clearing potential similar to that of the most effective clearing agents (e.g., sorbitol and fructose) in native skin.[5,9]

The ability to clear skin using 1,3-propanediol and 1,2-propanediol was evaluated for 1 and 24 h. RSR as a function of chemical agent concentration is shown for native rodent skin in Fig. 6. The slope from linear regression analysis of RSR data was used to define OCP for each chemical agent. ANCOVA was used to test the RSR data for statistically sig-

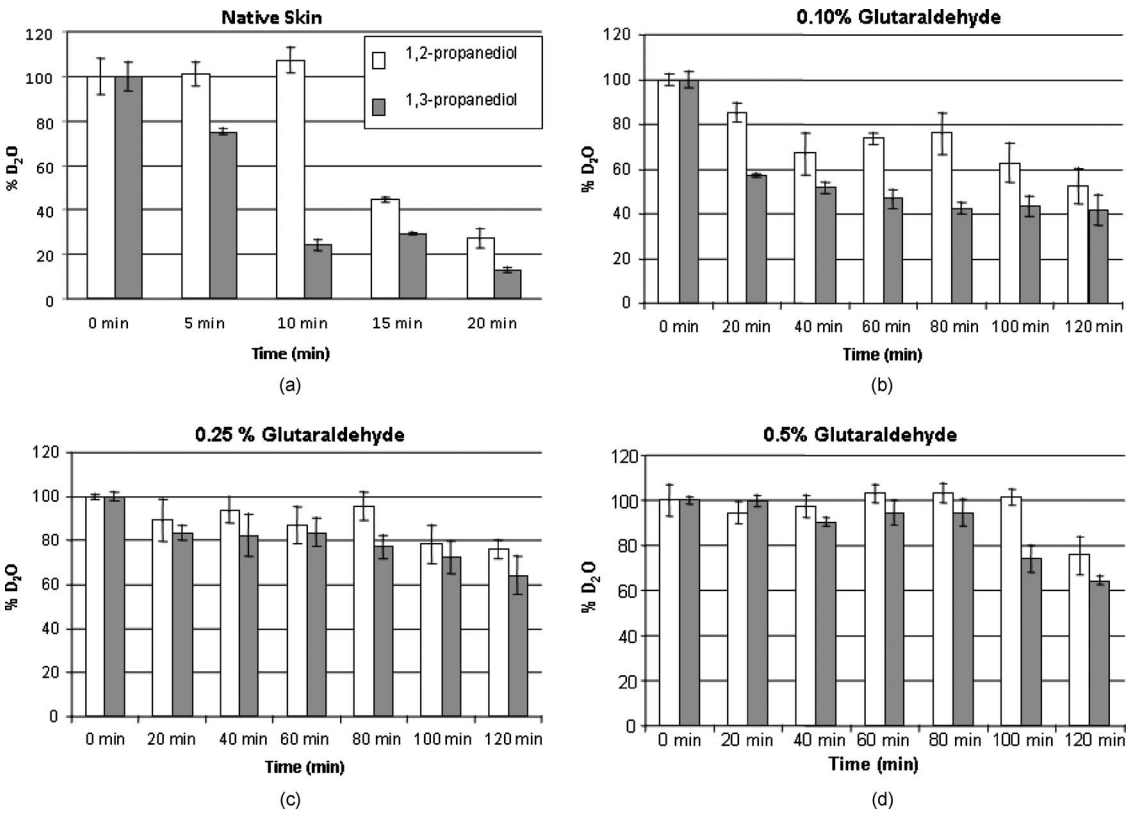

Fig. 4 Percent D_2O remaining after immersion in 1,2- and 1,3-propanediol for (a) native, (b) 0.10%, (c) 0.25%, and (d) 0.50% glutaraldehyde fixed skin.

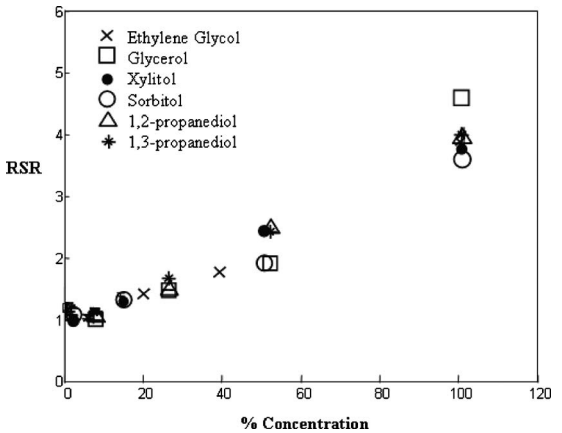

Fig. 5 Reduced scattering ratio as a function of agent concentration in 4% glutaraldehyde fixed skin after 24 h.

nificant differences in clearing ability. Consistent with our previous results,[5] a statistical difference in clearing efficacy was found between the propanediols (p value ≤ 0.05). After 1 h of clearing, 1,3-propanediol was found to be a more effective clearing agent than 1,2-propanediol with an OCP value of 0.406 versus 0.282. However, after 24 h, no differences in clearing were seen between 1,3- and 1,2-propanediol with OCP values of 0.433 and 0.392, respectively.

4 Discussion

This study builds on previous results that showed skin optical clearing induced by sugars and sugar alcohols correlated with collagen solubility.[5,9] OCP of these agents was shown to increase with molecular weight with an intriguing dependence on hydroxyl group position. In particular, 1,3-propanediol was shown to have twice the OCP of 1,2-propanediol even though they had identical molecular weights (76.10 Da), similar refractive index (1.44 versus 1.43), and osmolality (8.3 versus 8.7 Osm/kg).[5,9] The optical clearing potentials of 1,2- and 1,3-propanediol reflected those of analogous sugar alcohols ethylene glycol and glycerol, respectively, and suggested hydroxyl group position was an important factor in an agent's ability to induce skin clearing. Our simulation results clearly

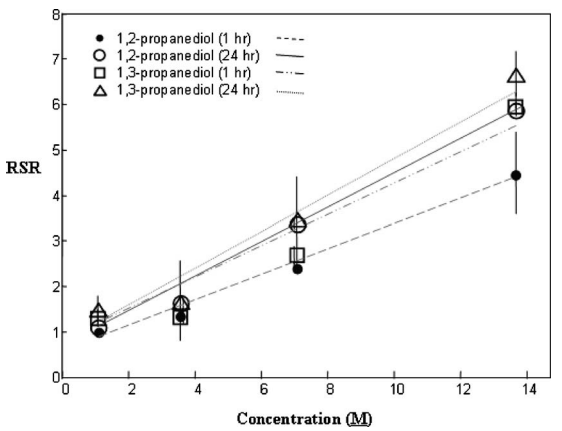

Fig. 6 RSR as a function of agent concentration in native skin after 1 and 24 h. Slope of linear regression lines indicates OCP.

indicate that the position of hydroxyl groups in alcohols affects their bridging ability. (Note that 1,2-propanediol and ethylene glycol can only form type I bridges, while 1,3-propanediol only forms type II bridges.) This suggestion was further supported by the result that xylitol (five carbon sugar alcohol) and glycerol (three carbon sugar alcohol) exhibited half the OCP of sorbitol (six carbons sugar alcohol), demonstrating that optical clearing was not solely dependent on molecular weight or the number of hydroxyl groups (as concluded in Ref. 28). Xylitol, like glycerol, preferentially forms type II rather than type IV bridges. This result provides a possible molecular basis for understanding similar OCP of xylitol and glycerol even though their molecular sizes are different. On the other hand, sorbitol preferred to form type IV bridges that span across the collagen surface and likely disrupt hydration layers more effectively. It should be noted that our previous experimental results reflected quasi-steady state conditions following 45 min of chemical agent exposures.[5,9] The present results suggest that the rate-limiting step in tissue optical clearing is the disruption of collagen hydration shell and that all the previously tested agents of the sugar and sugar alcohol series will eventually "clear" equally well given enough exposure time.

OCP of the sugar alcohols correlated with the preferred bridge type identified by our MD simulations, which is also consistent with what has been observed with nonlinear optical microscopy using second harmonic generation in collagenous tissues during tissue optical clearing.[7] Interactions that organize and assemble collagen molecules are mediated by hydration forces involving water bridges.[8] Earlier studies suggest that water bridges stabilize collagen tertiary structures and that hydration shell organizes triple helices for higher order assembly.[8,16,20] Characteristic of chemical agents with significant OCP is the ability to form hydrogen bond bridges, which would disrupt hydration layers and affect hydration forces mediating collagen self-assembly.

This molecular viewpoint of chemical agent-collagen interaction suggests that hindering the exchange of chemical agent with bound water would preserve the hydration layer, stabilize high-order collagen structures, and hinder tissue optical clearing. This can be accomplished by glutaraldehyde fixation, which has been corroborated by Raman spectroscopy studies using normal and deuterated water.[22] Glutaraldehyde fixation may reduce collagen conformational motion that slows water diffusion in and out of the collagen structure.[29] A similar experiment had been performed previously in which glycerol was observed to have a limited ability to induce transparency in formalin-fixed rodent skin and collagen gel.[7] In this study, Raman spectroscopy was used to assess the degree of water loss due to clearing agent exposure in native and fixed rodent skin tissue.

Consistent with previous works, Raman spectroscopy utilizing unique bands of deuterated water showed that glutaraldehyde fixation hindered water loss from exposure to a series of clearing agents (see Figs. 3 and 4). In particular, 1-h clearing agent exposures of rodent skin fixed in 0.1, 0.25, and 0.5% glutaraldehyde solutions showed increasing retention of water, and differences in water loss among exposures to ethylene glycol, glycerol and HFCS correlated with their OCP (Fig. 3).

The kinetics of dehydration were characterized using 1,2- and 1,3-propanediol. These agents were used because their similarity controlled for variables such as molecular weight, index of refraction, and osmolality. In native rodent skin, water loss with exposure to 1,3-propanediol was faster than when exposed to 1,2-propanediol, consistent with their respective OCPs [Fig. 4(a)]. This trend continued in fixed skin, but was less pronounced with higher glutaraldehyde concentration (Fig. 4). It should be noted that Raman signal was limited to the sample surface (which was measured from the dermal side), and therefore, data reflected water loss dynamics from the most superficial layers. However, we observed comparable water loss following long exposure times with both 1,2- and 1,3-propanediol in native and fixed skin. If this trend was consistent through the full thickness of tissue, then the induced transparency by clearing agents after long exposures should also be comparable, regardless of their respective OCP measured after 1-h exposures. This was indeed observed for a series of polyols applied for 24 h to glutaraldehyde-fixed rodent skin (Fig. 5). RSR was measured as a function of agent concentration and showed that after long exposure (24 h), all agents exhibited high OCP, equivalent to that of sorbitol in native skin.

Other classes of chemical agents such as dimethyl sulfoxide (DMSO)[30,31] have been shown to effectively clear tissue (with topical application) and exhibit collagen destabilization and solubilization. These observations are consistent with tissue optical clearing by disruption of collagen hydration shell, but achieved without hydrogen bond bridge formation. Similar to polyols, DMSO is amphiphilic with hydrophilic –S═O and hydrophobic methyl groups. Parametrized MD force field partial charge of the oxygen atom in DMSO (−0.556)[32] is weaker than that of oxygen atom in glycerol (−0.660), suggesting weaker association with collagen. However, instead of forming a hydrogen bond using the –S═O group, DMSO may also use the strongly hydrophobic methyl groups to bind to collagen and disrupt the hydration shell in a manner analogous to surfactants. Regardless of the details of molecular interactions, from what has been observed with DMSO,[30,31] it is likely that disruption of the hydration layer ultimately determines the efficacy of DMSO tissue optical clearing.

In summary, we submit that the optical clearing of collagenous tissue, by the homogenization of the refractive index, is dependent on the disruption of collagen hydration shell by chemical agent, which correlates with the agent's collagen solubility. As a consequence, collagen structure will be disrupted. Since fixed tissues could also be cleared, destabilization of collagen structure would be at the molecular level instead of affecting the meso-scale morphology of the collagen fiber network. As shown by previous studies, optical clearing does not show a dependence on agent refractive index, albeit over a limited range from 1.43 to 1.48, or osmolality, though presumably the agent should be hyperosmotic to facilitate bound water replacement.

The present results suggest that hyperosmotic agents will induce tissue optical clearing of equivalent magnitude (as measured by reduction in light scattering) given long-enough exposure times, at least in the *in vitro* setting. However, for potential biomedical applications, collagen solubility is an effective property with which to screen for chemical agents that induce the greatest reduction in tissue light scattering in the shortest amount of exposure time. It may come to pass that the index of refraction of effective clearing agents must fall within some range comparable to values reported for collagen (1.45–1.55). Further studies are needed to determine these limits.

5 Conclusions

MD simulations and optical spectroscopy were used to elucidate chemical agent interactions that drive (collagenous) tissue optical clearing. Tissue optical clearing is driven by the disruption and replacement of collagen hydration layer with a chemical agent. Hyperosmotic sugar and sugar alcohol solutions will induce equivalent temporary reduction in light scattering of native and fixed rodent skin, given a long-enough exposure time. However, the rate at which agent-induced optical clearing will occur depends on surface hydrogen bond bridge formation. This rate is correlated with occupation of collagen hydrogen bonding sites, with higher optical clearing rates for agents with preference for hydrogen bond bridge formation with hydroxyl groups at specific positional separation.

Ultimately, optical clearing must coincide with homogenization of tissue refractive index. The present results suggest that this homogenization is rate limited by disruption of the collagen hydration shell by chemical agent. Optical clearing results from long exposure time of native and fixed skin to polyols exhibited no dependence on agent index of refraction, albeit over a limited range (1.43–1.48). A necessary property is that the chemical agent be hyperosmotic to tissue, where the most effective ones will be a subset that exhibit high rates of collagen hydration layer disruption and replacement. These agents may be screened by their collagen solubilities.

Acknowledgments

The authors thank Ryan Byrd and Krystle Page from the Laboratory Animal Research and Resources (LARR) facility at Texas A&M University and the Archer Daniels Midland Company for samples of HFCS. This work was funded in part by a National Science Foundation Faculty Early Career Development (CAREER) Award (A.T.Y.). The Raman spectroscopy system from the Materials Characterization Facility at Texas A&M was funded by a National Science Foundation Grant (No. BES-0421409).

References

1. V. V. Tuchin, *Optical Clearing of Tissues and Blood*, SPIE, Bellingham, WA (2005).
2. G. Vargas, E. K. Chan, J. K. Barton, H. G. Rylander, III, and A. J. Welch, "Use of an agent to reduce scattering in skin," *Lasers Surg. Med.* **24**, 133–141 (1999).
3. C. G. Rylander, O. Stumpp, T. Milner, N. J. Kemp, and J. M. Mendenhall, "Dehydration mechanism of optical clearing in tissues," *J. Biomed. Opt.* **11**(4), 041117 (2006).
4. V. V. Tuchin, R. K. Wang, and A. T. Yeh, "Optical clearing of tissues and cells," *J. Biomed. Opt.* **13**, 021101 (2008).
5. J. M. Hirshburg, B. Choi, J. S. Nelson, and A. T. Yeh, "Collagen solubility correlates with skin optical clearing," *J. Biomed. Opt.* **11**(4), 040501 (2006).
6. L. Leonardi, A. Ruggeri, N. Roveri, A. Bigi, and E. Reale, "Light microscopy, electron microscopy, and x-ray diffraction analysis of glycerinated collagen fibers," *J. Ultrastruct. Res.* **85**, 228–237 (1983).

7. A. T. Yeh, B. Choi, J. S. Nelson, and B. J. Tromberg, "Reversible dissociation of collagen in tissues," *J. Invest. Dermatol.* **121**(6), 1332–1335 (2003).
8. N. Kuznetsova, S. L. Chi, and S. Leikin, "Sugars and polyols inhibit fibrillogenesis of type I collagen by disrupting hydrogen-bonded water bridges between the helices," *Biochemistry* **37**, 11888–11895 (1998).
9. J. Hirshburg, B. Choi, J. S. Nelson, and A. T. Yeh, "Correlation between collagen solubility and skin optical clearing using sugars," *Lasers Surg. Med.* **39**, 140–144 (2007).
10. M. P. Allen and D. J. Tildesley, *Computer Simulation of Liquids*, Clarendon Press, New York (1987).
11. B. R. Brooks, C. L. Brooks, 3rd, A. D. Mackerell, Jr., L. Nilsson, R. J. Petrella, B. Roux, Y. Won, G. Archontis, C. Bartels, S. Boresch, A. Caflisch, L. Caves, Q. Cui, A. R. Dinner, M. Feig, S. Fischer, J. Gao, M. Hodoscek, W. Im, K. Kuczera, T. Lazaridis, J. Ma, V. Ovchinnikov, E. Paci, R. W. Pastor, C. B. Post, J. Z. Pu, M. Schaefer, B. Tidor, R. M. Venable, H. L. Woodcock, X. Wu, W. Yang, D. M. York, and M. Karplus, "CHARMM: the biomolecular simulation program," *J. Comput. Chem.* **30**(10), 1545–1614 (2009).
12. W. Im, M. S. Lee, and C. L. Brooks, "Generalized born model with a simple smoothing function," *J. Comput. Chem.* **24**, 1691–1702 (2003).
13. J. A. Ramshaw, N. K. Shah, and B. Brodsky, "Gly-X-Y tripeptide frequencies in collagen: a context for host-guest triple-helical peptides," *J. Struct. Biol.* **122**(1–2), 86–91 (1998).
14. N. K. Shah, J. A. Ramshaw, A. Kirkpatrick, C. Shah, and B. Brodsky, "A host-guest set of triple-helical peptides: stability of Gly-X-Y triplets containing common nonpolar residues," *Biochemistry* **35**(32), 10262–10268 (1996).
15. R. Z. Kramer, J. Bella, P. Mayville, B. Brodsky, and H. M. Berman, "Sequence dependant conformational variations of collagen triple-helical structure," *Nat. Struct. Biol.* **6**, 454–457 (1999).
16. K. M. Ravikumar and W. Hwang, "Region-specific role of water in collagen unwinding and assembly," *Proteins* **72**, 1320–1332 (2008).
17. J. K. Rainey and M. C. Goh, "An interactive triple-helical collagen builder," *Bioinformatics* **20**, 2458–2459 (2004).
18. A. T. Brunger and M. Karplus, "Polar hydrogen positions in proteins: empirical energy placement and neutron diffraction comparison," *Proteins* **4**, 148–156 (1988).
19. D. Anderson, "Collagen self-assembly: a complementary experimental and theoretical perspective," Ph.D. thesis, University of Toronto (2005).
20. K. M. Ravikumar, J. D. Humphrey, and W. Hwang, "Spontaneous unwinding of a labile domain in a collagen triple helix," *J. Mech. Mater. Struct.* **2**, 999–1010 (2007).
21. H. De Loof, L. Nilsson, and R. Rigler, "Molecular dynamics simulation of galanin in aqueous and nonaqueous solution," *J. Am. Chem. Soc.* **114**, 4028–4035 (1992).
22. M. Jastrzebska, R. Wrzalik, A. Kocot, J. Zalewska-Rejdak, and B. Cwalina, "Hydration of glutaraldehyde-fixed pericardium tissue: raman spectroscopic study," *J. Raman Spectrosc.* **34**, 424–431 (2003).
23. M. Jastrzebska, R. Wrzalik, A. Kocot, J. Zalewska-Rejdak, and B. Cwalina, "Raman spectroscopic study of glutaraldehyde-stabilized collagen and pericardium tissue," *J. Biomater. Sci.* **14**, 185–197 (2003).
24. J. W. Pickering, S. Prahl, N. van Wieringen, J. B. Beek, H. J. C. M. Sterenborg, and M. van Gemert, "Double integrating sphere system for measuring optical properties of tissue," *Appl. Opt.* **32**, 399–410 (1993).
25. S. A. Prahl, "The adding-doubling method," Chapter 5 in *Optical-Thermal Response of Laser Irradiated Tissue*, A. J. Welch and M. J. C. van Gemert, Eds., pp. 101–129, Plenum Press, Portland (1995).
26. B. Rosner, *Fundamentals of Biostatistics*, Duxbury Thomas Learning, Pacific Grove, CA (2000).
27. A. T. Yeh and J. Hirshburg, "Molecular interactions of exogenous chemical agents with collage—implications for tissue optical clearing," *J. Biomed. Opt.* **11**(1), 014003 (2006).
28. Z. Mao, D. Zhu, Y. Hu, X. Wen, and Z. Han, "Influence of alcohols on the optical clearing effect of skin *in vitro*," *J. Biomed. Opt.* **13**(2), 021104 (2008).
29. D. T. Cheung, N. Perelman, E. C. Ko, and M. E. Nimni, "Mechanism of crosslinking of proteins by glutaraldehyde III. Reactions with collagen in tissues," *Connect. Tissue Res.* **13**, 109–115 (1985).
30. A. K. Bui, R. A. McClure, J. Chang, C. Stoianovici, J. Hirshburg, A. T. Yeh, and B. Choi, "Revisiting optical clearing with dimethyl sulfoxide (DMSO)," *Lasers Surg. Med.* **41**(2), 142–148 (2009).
31. M. Zimmerley, R. A. McClure, B. Choi, and E. O. Potma, "Following dimethyl sulfoxide skin optical clearing dynamics with quantitative nonlinear multimodal microscopy," *Appl. Opt.* **48**(10), D79–87 (2009).
32. M. L. Strader and S. E. Feller, "A flexible all-atom model of dimethyl sulfoxide for molecular dynamics simulations," *J. Phys. Chem. A* **106**, 1074–1080 (2002).